13

Structural changes and depth redistribution of implanted In and As dopants in Si during steady-state and pulsed heat treatment

© R.I. Batalov,[1] V.V. Bazarov,[1] E.M. Begishev,[1] V.F. Valeev,[1] V.I. Nuzhdin,[1] F.F. Komarov,[2] I.K. Chupris[2]

[1]Zavoisky Physical-Technical Institute — a standalone subdivision of the Federal Research Center „Kazan Scientific Center of the Russian Academy of Sciences“,
420029 Kazan, Russia
[2]Sevchenko Institute of Applied Physical Problems of Belarusian State University,
220045 Minsk, Belarus
e-mail: batalov@kfti.knc.ru

Received November 21, 2025
Revised December 10, 2025
Accepted December 15, 2025

Formation of nanoparticles of narrow-bandgap indium arsenide (InAs) in a subsurface region of single crystal silicon (Si) is one of approaches to extend optical absorption and a photoresponse of Si to the near- and mid-infrared range ($\lambda = 1.1-3.5\,\mu$m). The InAs nanoparticles can be synthesized by High-Dose Ion Implantation with subsequent steady-state or pulsed annealing. Rutherford Backscattering of helium ions was used to study a depth distribution of a concentration of the introduced dopant and a location of subsequently implanted ions In^+ (30 keV, $2 \cdot 10^{16}$ cm^{-2}) and As^+ (25 keV, $2 \cdot 10^{16}$ cm^{-2}) in the Si crystal lattice before and after various thermal impacts in solid-phase and liquid-phase modes. We have found thermal impact modes, at which the disturbed Si crystal structure is restored in the best way and conditions are created for synthesis of the InAs phase with the highest overlapping of profiles of the concentrations of the dopant atoms.

Keywords: silicon, indium arsenide, melting, crystallization, diffusion, segregation, Rutherford backscattering.

DOI: 10.61011/TP.2026.04.63277.318-25

Introduction

Due to its band structure with the band gap of $E_g = 1.12$ eV, the crystalline Si has a high level of optical absorption in the spectrum range $\lambda = 0.3-1.0\,\mu$m, but at the same time it very weakly absorbs light in the near- and mid-infrared range ($\lambda = 1.1 \cdot 10\,\mu$m) [1]. For this reason, Si is widely applied in optoelectronics for creating *p*- and *p*-*i*-*n*-photodiodes for the UV, visible and mid-infrared range (the photoresponse edge is up to $1.1\,\mu$m) and for solar cells. At the same time, structures of the silicon solar panels are transparent for an infrared part of the solar spectrum, which is $\sim 30\,\%$ of a total flux of sun energy [2]. In a longer wavelength range, narrow-bandgap materials ($E_g = 0.1-0.7$ eV) such as Ge, InAs, InSb [3], PbS [4] and CdHgTe [5] are applied, whose layer formation is poorly compatible with a traditional silicon planar technology. When growing these materials on the single-crystal Si substrate, there are difficulties related to a noticeable difference of lattice parameters and thermal expansion coefficients of the layer and the substrate, thereby causing formation of mechanical stresses of dislocations and high leakage currents in instrument structures.

A promising approach to expansion of Si functional capabilities to the near- and mid-infrared range is to create composite Si structures with the A_3B_5 nanoparticles by Ion-Beam Synthesis. This method includes high-dose implantation of the dopant elements of the III and V groups into Si for a specified depth with subsequent thermal annealing at the temperatures $T = 800\,^\circ$C$-1100\,^\circ$C in order to restore the disturbed crystal structure and to stimulate nucleation and growth of the nanoparticles [6–9]. It should be noted that the said method is well compatible with the traditional silicon technology and widely used in microelectronics when creating buried insulating (SiO_2, Si_3N_4) and semiconductor (SiC, SiGe) layers.

An alternative to steady-state (equilibrium) thermal annealing in a furnace in the solid-phase mode can be pulsed annealing in a nanosecond (laser and ion beams) or a millisecond-second (halogen and xenon lamps) range to be usually performed in the liquid-phase mode with formation of a melt on a surface. Fast processes of melting and subsequent crystallization ($V \sim 1-5$ m/s) from the undisturbed single-crystal substrate facilitate formation of epitaxial layers with lower defectiveness and a higher content of the dopant in a node (electrically-active) position in the crystal lattice [10].

It has been recently reported that pulsed laser annealing (PLA) is applied for the first time to the Si layers enriched with the high-energy ions In^+ and As^+ [11]. Both the nanosecond ($\tau = 70$ ns) and the millisecond ($\tau = 0.4$ ms) pulses of a ruby laser ($\lambda = 694$ nm) were used in the liquid-phase and the solid-phase modes of annealing, respectively. It has been demonstrated with application of Rutherford Backscattering (RB) that the solid-phase mode is characterized by full recrystallization of the enriched Si layer (a crystallinity degree is 25 %) with a 19 % portion of the dopant atoms in a substitution position f. At the same time,

the authors of the study [11] observed significant diffusion of both the dopants to the surface and heavy segregation in the thin Si layer (10−20 nm). For comparison, the liquid-phase mode of annealing (with formation of the melt of the thickness of up to 0.4 μm) is characterized by higher-quality restoration of the Si lattice (the crystallinity parameter was up to 47 %) and a higher substitution level (the parameter f was up to 35 %). At the same time, significant diffusion of the dopant (mainly As) deep into Si was observed at the melt stage.

The authors of the present study have recently reported pulsed ion annealing (PIA) by a powerful beam of the ions C^+/H^+ to the Si layers enriched with the low-energy ions In^+ and Sb6+ [12]. This method of annealing does not depend on optical properties of the material and is characterized by a more uniform (as compared to PLA) depth distribution of energy, a higher thickness of the melt ($\sim 1\,\mu$m) and a higher treatment area per pulse (a spot diameter is about 2 cm). It was demonstrated that during PIA a capture of the dopant atoms to the node positions was 30 %, while a structural perfection level was 54 %. At the same time, we also observed diffusion of the Sb atoms deep into Si. Results of study of a phase composition of the irradiated layers indicate that the InSb phase is formed.

The present study is aimed at determining influence of various kinds of thermal treatment: steady-state thermal annealing (TA) in the furnace, nanosecond PLA and PIL as well as fast thermal annealing (FTA) of second duration on the depth distribution of the concentration of the atoms In and As in Si, their positions in the Si lattice as well as on restoration of crystallinity of the doped layer.

1. Experiment

The substrate for ion implantation was a plate of single-crystal Si of the p-type of conduction with the orientation (111), the thickness of 350 μm with resistivity of 20 Ω·cm (KDB-20). Before implantation, a natural oxide layer was removed from a surface of the Si plate in a hydrofluoric acid aqueous solution with flushing in distilled water. The plate p-Si was subsequently enriched with the ions In^+ first and then the ions As^+, which were produced from an InAs powder, in an ion-beam accelerator ILU-3. The energy of the ions In^+ was $E = 30$ keV, while the energy of the lighter ions As^+ was selected to be 25 keV in order to provide overlapping of the concentration profiles of the introduced atoms along the depth. The dose of each type of the ions was $D = 2 \cdot 10^{16}$ ion/cm^2 with the density of the ion current $j = 2\,\mu$A/cm^2. In order to prevent heating of the samples the ions were implanted with water cooling of a steel cassette with the samples.

For crystallization of the subsurface Si region amorphized with ion irradiation, various types of thermal treatment were performed. Table 1 shows a list of the produced samples and indicates modes of the thermal treatement. The initial sample K1 was produced only by ion implantation without annealing. The K2 sample was subjected to PIA in the pulse ion accelerator TEMP-2M, which generated the powerful ion beam with the following parameters: the composition of the ion beam $\approx 80\,\%$ C^+, $\approx 20\,\%$ H^+, the maximum energy of the ions $E \approx 300$ keV, duration of the pulse $\tau \approx 100$ ns, the pulse energy density $W \approx 1.0$ J/cm^2, fluence of the ions C^+/H^+ per pulse $D \approx 10^{13}$ ion/cm^2. The K3 sample was subjected to PLA in air by means of a neodymium glass pulse laser. We used radiation of the second harmonic at the wavelength $\lambda = 532$ nm with pulse duration $\tau = 10$ ns with the comparable energy density. PLA was performed with partial overlapping of the laser spots of the size of 4 mm. The samples K4a and K4b were produced during TA in the quartz furnace in a nitrogen flow at the temperatures $T = 800\,^\circ$C and 1000 °C, respectively, for 30 min. The K5 sample was produced during FTA with halogen lamps of power of 1 kW each in an upgraded unit „Impul's-6". The sample temperature was kept near a melting point of Si ($\approx 1400\,^\circ$C) for 5 s.

The depth distribution of the concentration of the introduced dopants In and As in Si, their position in the Si lattice and the crystallinity degree of the modified Si layer were studied by means of Rutherford Backscattering. The RB spectra were recorded in an acceleration system AN-2500 in modes of channeling (RB/C) of the ions along the direction (111) of the SI crystals and by shooting a random (unoriented) spectrum (RB/R) using the ions He^+ with the energy of 1.5 MeV at a recording angle of 170°. The dopant profiles were calculated from the RB spectra by means of a software package HEAD-6 designed in Sevchenko Institute of Applied Physical Problems of Belarusian State University and of SIMNRA [13]. Theoretical distributions of the concentration of the implanted atoms In and As before thermal treatment were calculated using the SRIM software [14].

2. Results and discussion

Fig. 1, a shows the experimental RB spectra of the K1 sample, which are shot in the random and channeled modes, as well as the simulated RB spectrum of the enriched sample. We note that a depth scale is proportional to a scale of energy channels in the RB spectra, but is an opposite direction. The dopant region of the spectrum (the channel region 390−460) exhibits two mutually separated intense peaks, which correspond to As (the channels 400−420) and heavier In (the channels 430−460). We note that an area of the As peak is significantly smaller than an area of the In peak despite the same dose of implantation for both the dopants. This difference is caused by a higher scattering cross section of the ions He+ on the heavy In atoms that are near the sample surface. A projective path of the ions In^+ for 30 keV is estimated to be $R_p = 23$ nm with a standard deviation $\Delta R_p = 6$ nm (without taking into account Si sputtering) according to data of the SRIM software [14].

Table 1. List of the produced samples and their annealing modes

Sample number	Annealing type	Annealing mode
K1	Without annealing	–
K2	Pulsed ion one	C^+/H^+, $E = 300$ keV, $\tau = 100$ ns, $W \approx 1.0$ J/cm^2, vacuum
K3	Pulsed laser one	$\lambda = 532$ nm, $\tau = 10$ ns, $W = 1.0$ J/cm^2, air
K4a	Thermal one (in the furnace)	$T = 800\,^\circ$C, $t = 30$ min, N_2
K4b	Thermal one (in the furnace)	$T = 1000\,^\circ$C, $t = 30$ min, N_2
K5	Fast lamp one	$T \approx 1400\,^\circ$C, $t = 5$ s, air

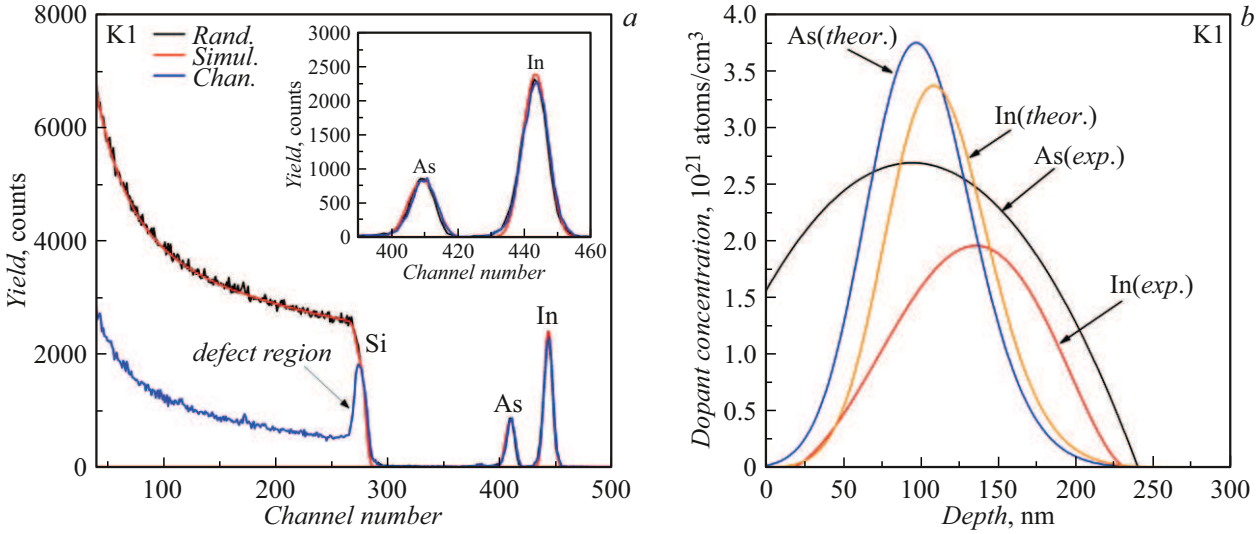

Figure 1. Experimental (random — the black curve, channeled — the blue curve) and simulated (random — the red curve) RB spectra of the K1 sample (a), the theoretical (In — the orange curve, As — the blue curve) and experimental (In — the red curve, As —the black curve) profiles of the concentrations of the atoms In and As in Si in the K1 sample (b).

In the region of the Si substrate (the channels with the numbers below 300), the channeled spectrum has a sharp peak that characterizes disordering of the SI lattice near the surface (amorphization). The width of this peak is comparable to widths of the dopant peaks. Coincidence of the spectra for the dopant atoms, which are shot under conditions of channeling of the helium ions and in the unoriented mode (the insert of Fig. 1, a), also indicates an amorphous state of the ion-enriched Si layer.

Fig. 1, b shows the calculated and experimental concentration profiles after ion implantation. The experimental profiles are obtained by simulating the RB/R spectra till the best coincidence with the measured spectra. It should be noted that under the conditions of high-dose ion implantation, due to the effect of radiation-induced diffusion of the dopant atoms we observe noticeable redistribution of their concentration both into the depth to the region of „end-of-range“ defects as well as towards the surface (Fig. 1, b). Sputtering of the sample surface during irradiation by the heavy ions of In and As results in a quite large change of the distributions of the dopant concentration in the subsurface region, especially, of the In atoms. Results of the measurements indicate a wide region of overlapping of the concentration distributions of the introduced dopants.

In order to estimate the crystallinity degree of the irradiated Si layer and a degree of substitution of the Si atoms with the dopant atoms In and A in the nodes of the crystal lattice, we have applied parameters $f_{cr}(\%)$ and $f_{im}(\%)$, which are respectively defined as yields of the channeled spectrum (RB/C) to the random (unoriented) one (RB/R) within a dopant embedment region. For Si, the analyzed region corresponded to the channels 170–300, so did it to the channels 310–460 for the dopants In and As. Expressions for $f_{cr}(\%)$ and $f_{im}(\%)$ are taken from the study [11] and written as:

$$f_{cr}(\%) = (1 - \chi^{Si})/(1 - \chi^{min}),$$

$$f_{im}(\%) = (1 - \chi^{In+As})/(1 - \chi^{min}).$$

Here, χ^{Si} and χ^{In+As} are the above-said ratios and χ^{min} is a relationship for the qualitative (initial) silicon lattice, which is 0.05. For the fully amorphous sample, χ^{min} will be unity.

Table 2. Crystallinity degree of the silicon layers (f_{cr}) and the portion of the dopant in the nodes of the crystal lattice (f_{im}) after double implantation of the ions of In and As and various thermal treatments

Sample number	Silicon yield (channels 170–300)		Dopant yield (In+As) (channels 320–460)	
	$1-\chi^{Si}$	$f_{cr}(\%)$	$1-\chi^{In+As}$	$f_{im}(\%)$
K1	0.718	75.6	0.009	1.0
K2	0.725	76.3	0.242	25.5
K3	0.707	74.4	0.298	31.4
K4a	0.823	86.6	0.214	22.5
K4b	0.821	86.4	0.426	44.8
K5	0.837	88.1	0.236	24.8

The results of calculation of the said parameters for the enriched Si sample in the K1 sample are given in Table 2. They were $f_{cr} = 75.6\,\%$ and $f_{im} = 1\,\%$, thereby indicating a quite high crystallinity degree due to the thin disturbed layer (≈ 70 nm) within the analyzed region and a very low degree of dopant substitution (the large part of the dopant atoms is probably concentrated in interstice and/or clusters).

Below we consider an effect of various thermal treatments on a behavior of the implanted dopants in Si. Fig. 2, *a* shows the RB spectra of the K2 sample produced after double implantation and PIA. It is clear that the peaks of As and In became almost indistinguishable to form a unified peak with a tail extended deep into the sample (the more noticeable separation of the peaks is observed in the insert of Fig. 2, *a* for the channeled spectrum). This type of the RB spectrum is caused by melting of the subsurface region of the sample during pulsed annealing and diffusion of the introduced dopants in the melt. According to the calculated data [15], when the powerful ion beam of nanosecond duration with $W = 1.0\,\mathrm{J/cm^2}$ affects a two-layer structure a-Si(0.1 μm)/c-Si(350 μm), a melt depth in the beam center can be up to 0.8 μm (twice as high as that during PLA [11]), a melt lifetime can be up to about 400 ns and the maximum temperature on the surface can be up to about 1700 °C.

The measurements in the channeling mode within the dopant range of the spectrum demonstrated reduced yield of helium ions around the In peak and a significant drop around the As peak, i.e. a part of atoms of both the sorts takes a substitutional position in the Si lattice. Taking into account reference data about maximum equilibrium solubility of these dopants in solid Si ($6 \cdot 10^{19}$ atoms/cm^3 for In and $1.5 \cdot 10^{21}$ atoms/cm^3 for As [16]) and their behavior during pulsed treatment [11,12], we can assume that in our case the IN atoms after diffusion in the melt are highly displaced to the surface by a moving front of melt crystallization (the segregation effect). At the same time, the As dopant that is more soluble in Si actively diffuses deep into Si at the melt stage and is incorporated into the nodes of the Si lattice at the stage of its solidification without being highly displaced. As to the silicon range of the RB/C spectrum, it exhibits full disappearance of the amorphous layer, thereby indication restoration of the crystal structure of the layer up to an epitaxial one. The RB spectra in Fig. 2, *a* were analyzed in detail to demonstrate that the crystallinity degree of the annealed Si layer in the K2 sample is 76.3 %, while the portion of the dopant atoms in the substitution position sharply increases to 25.5 % (Table 2).

Fig. 2, *b* shows the experimental profiles of In and As in Si after PIA. By comparing the simulated spectrum and the experimental spectrum, the distributions of the concentrations of both the dopants are separated. It is clear that the introduced dopants have been intensively diffusionally distributed deep into SI up to 600–650 nm, but there is also their accumulation near the Si surface (segregation), which for the In atoms is in 4 times higher (up to $2 \cdot 10^{21}$ atoms/cm^3) than for As. It can be concluded based on this figure that the deep region of the sample (100–650 nm) has a high-concentration solid solution formed, in which the As atoms predominantly occupy the node positions, while near the surface there are conditions being created for forming the metal In nanoparticles. The In concentration at the depths 200–500 nm noticeably exceeds a limit of equilibrium solubility, while the concentration of the As atoms is noticeably lower than a limit of equilibrium solubility for this dopant. Formation of the InAs in this sample seems unlikely. It can be taken into account after calculating the portion of the dopant in the node position.

Below we consider impact of nanosecond laser pulses on the enriched Si (the K3 sample). The results of PLA when $W = 1.0\,\mathrm{J/cm^2}$ are shown in Fig. 3. It is clear from the RB data in the dopant region of the spectra (Fig. 3, *a*) that the peaks of In and As are weakly overlapped and widened deep into Si and towards the surface thereof. The channeled spectrum of the sample (the insert of Fig. 3a) shows largely reduced yield of the ions H+ in both the dopant peaks, thereby indicating intense incorporation of the dopant atoms into the nodes of the Si lattice. At the same time, the subsurface Si region exhibits a clear peak (the channels 250–290), which indicates residual defectiveness in the layer. Its nature can be caused both by presence of an amorphous or a polycrystalline fraction in this layer as well as by formation of nanoparticles of a secondary InAs phase. In this case, the crystallinity degree of the Si layer is 74.4 %, while the portion of the dopant atoms in the substitution position increases to 31.4

The experimental profiles of the concentration of the dopant atoms In and As in Si after PLA are shown in Fig. 3, *b*. It can be noted that the profiles are similar in a shape and have a slight difference in the peak concentration ($2.1 \cdot 10^{21}$ atoms/cm^3 for As and $1.7 \cdot 10^{21}$ atoms/cm^3 for In). The profiles extend as far as the depth of 450 nm, thereby indicating melting of the Si layer during PLA for this depth, and it complies with our calculated data. Almost complete overlapping of the dopant profiles and a high

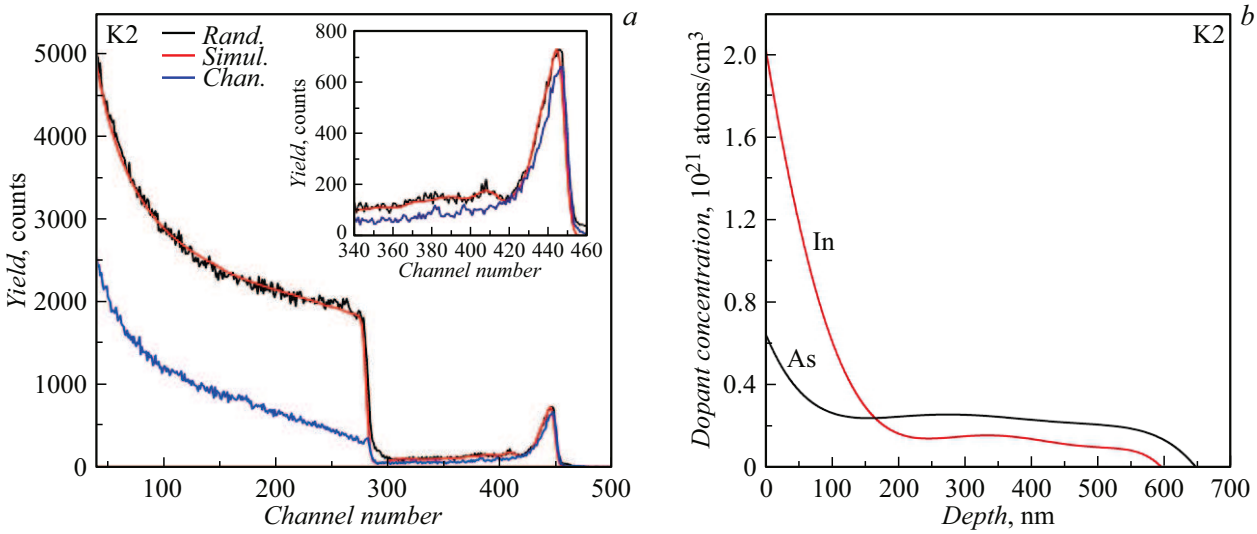

Figure 2. Experimental (random — the black curve, channeled — the blue curve) and simulated (random — the red curve) RB spectra of the K2 sample (*a*) and the obtained experimental profiles of the concentrations of the atoms of In (the red curve) and As (the black curve) in Si in the K2 sample (*b*).

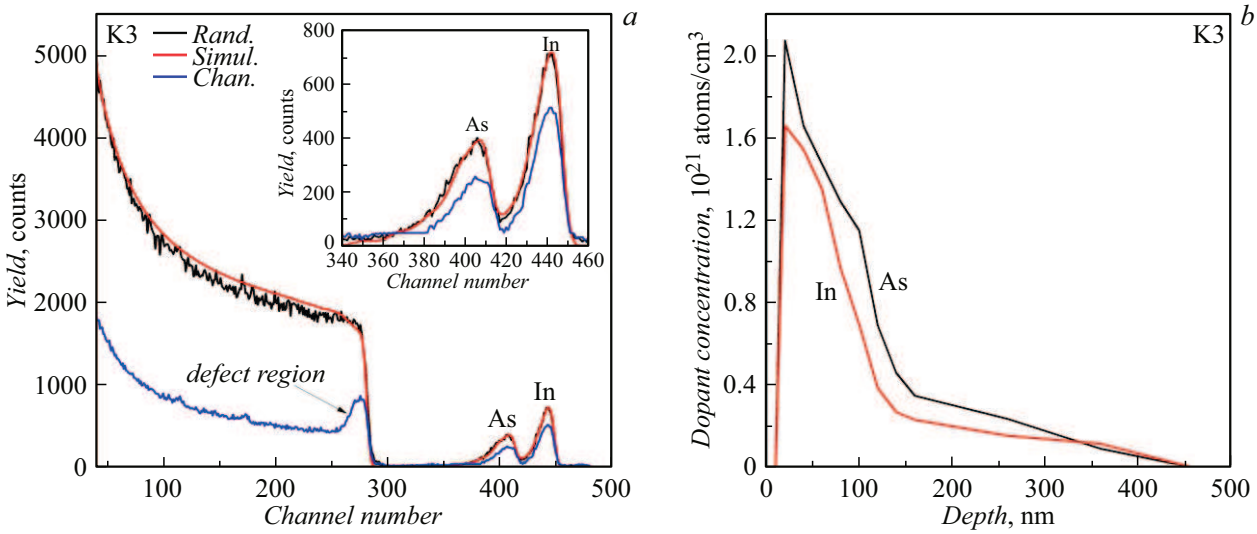

Figure 3. Experimental (random — the black curve, channeled — the blue curve) and simulated (random — the red curve) RB spectra of the K3 sample (*a*) and the obtained experimental profiles of the concentrations of the atoms of In (the red curve) and As (the black curve) in Si in the K3 sample (*b*).

concentration of the atoms of the both the sorts in the layer up to 100 nm create conditions for nucleation of the InAs-phase nanoparticles in this region.

Now we proceed to consideration of influence of steady-state (equilibrium) annealing on the profiles of the dopants In and As in Si. Fig. 4, *a* shows the RB spectra for the K4a sample after annealing in the furnace at 800 °C/30 min. In the dopant region of the spectrum, the peaks of In and As practically retain their original shape. Slight widening deep into Si is observed for the In peak. The channeled spectrum exhibits reduced yield of helium ions, which is more noticeable for the As atoms than for the In atoms. It should be noted in the silicon range that there is an oxygen peak (the 174 channel), which indicates formation of a thin silicon oxide layer, and its respective weak peak near the Si surface, which indicates residual defectiveness in the layer. After such annealing, the crystallinity degree of the Si layer in the K4a sample increases to 86.6 %, while the portion of the dopant atoms in the substitution position is 22.5 % (Table 2).

The experimental concentration profiles of the dopants (Fig. 4, *b*) exhibit a shift of the In profile towards the surface with the peak concentration of $6.1 \cdot 10^{21}$ atoms/cm^3 and a certain shift of the As profile deep into Si at the peak concentration of $4 \cdot 10^{21}$ atoms/cm^3. Thus, the conditions for formation of the InAs nanoparticles are created in the

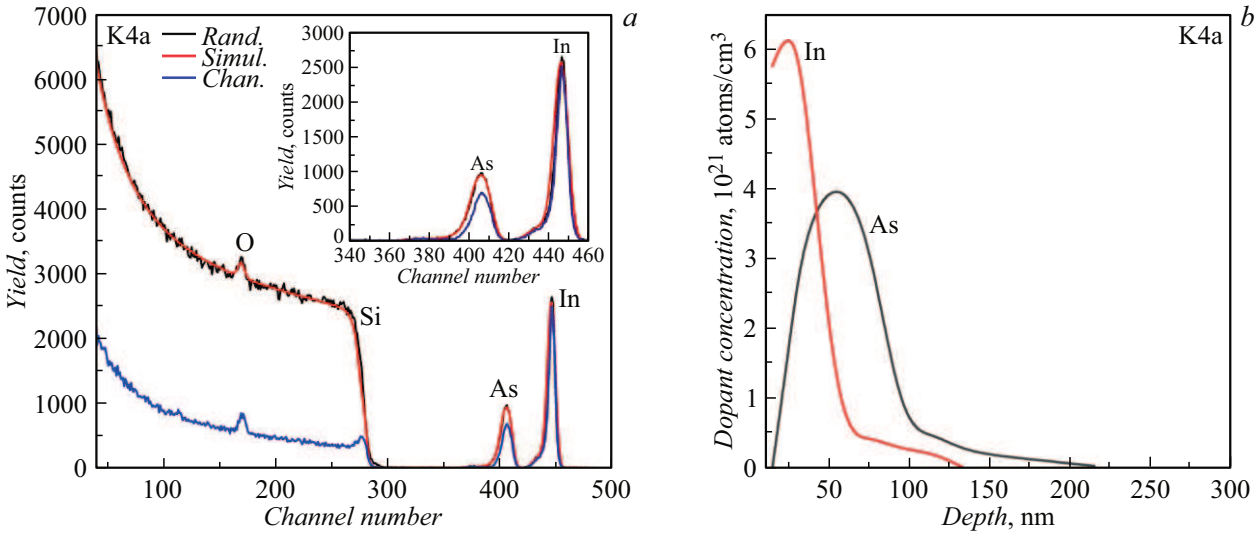

Figure 4. Experimental (random — the black curve, channeled — the blue curve) and simulated (random — the red curve) RB spectra of the K4a sample (*a*) and the obtained experimental profiles of the concentrations of the atoms of In (the red curve) and As (the black curve) in Si in the K4a sample (*b*).

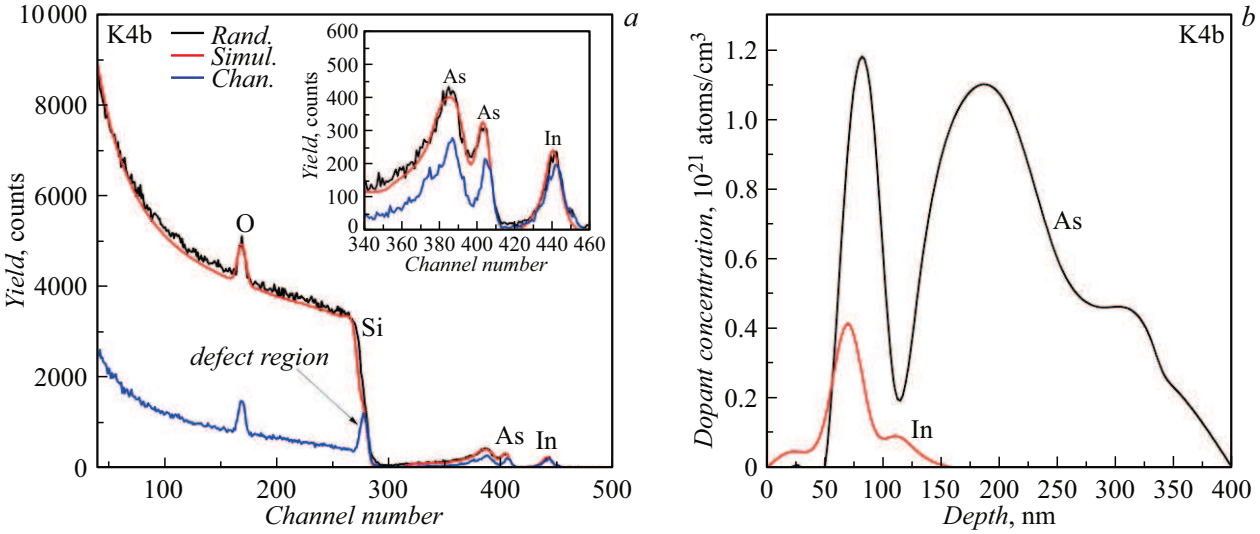

Figure 5. Experimental (random — the black curve, channeled — the blue curve) and simulated (random — the red curve) RB spectra of the K4b sample (*a*) and the obtained experimental profiles of the concentrations of the atoms of In (the red curve) and As (the black curve) in Si in the K4b sample (b).

subsurface layer of the 50 nm thickness, where the highest content of the dopants In and As is concentrated.

The increase of the annealing temperature to 1000 °C (the K4b sample) results in a significant change of the RB spectrum in the dopant region (Fig. 5, *a*). It is clear that intensity of the In peak largely drops, while the As peak bifurcates and demonstrates escape of the dopant deep into Si. The channeled spectrum demonstrates slight reduction of yield of helium ions in the In peak and a higher drop of yield in the As peak in both the cases due to the node position of the introduced dopant. The silicon region exhibits the increase of intensity of the oxygen peak, while measurements in the channeling mode indicate presence of a thin disordered region near the surface. Despite the high temperature of annealing, such disordering is caused by presence of the amorphous SiO_2 film on the Si surface along with possible formation of the InAs nanoparticles, which was observed in the literature [6,9]. After annealing at 1000 °C in the K4b sample, the crystallinity degree of the Si layer is 86.4 %, while the portion of the dopant atoms in the substitution position gets the maximum value of 44.8 % (Table 2).

The experimental dopant concentration profiles (Fig. 5, *b*) demonstrate a drop of intensity of the In peak due to its

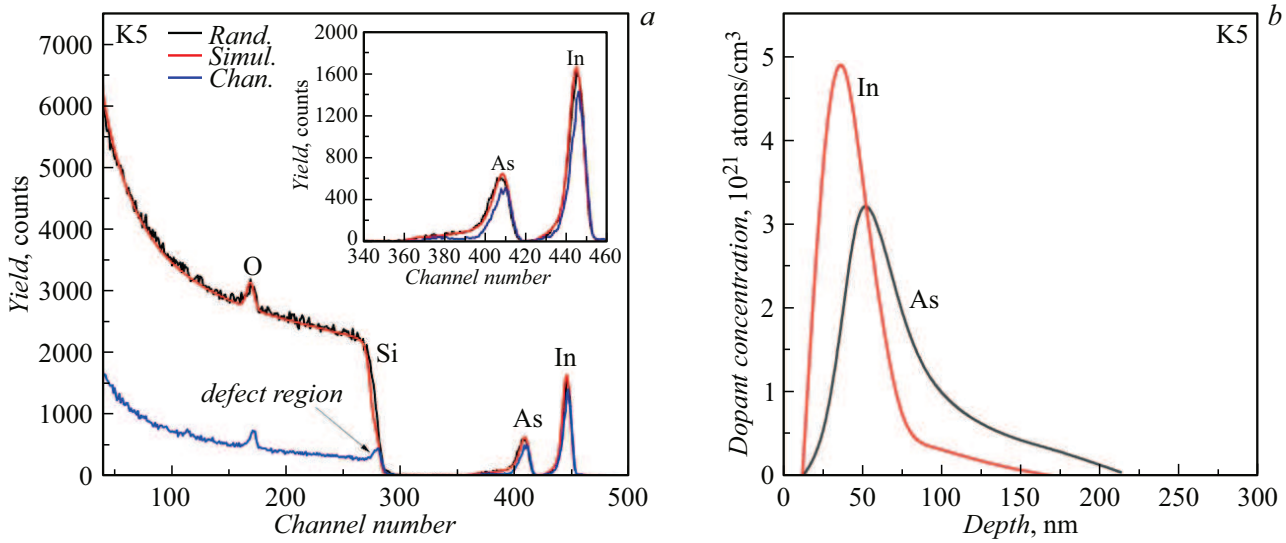

Figure 6. Experimental (random — the black curve, channeled — the blue curve) and simulated (random — the red curve) RB spectra of the K5 sample (*a*) and the obtained experimental profiles of the concentrations of the atoms of In (the red curve) and As (the black curve) in Si in the K5 sample (*b*).

evaporation to the concentration level of $4 \cdot 10^{20}$ atoms/cm^3 at the depth of 70 nm with tail regions towards the surface and deep into Si. The As atoms are almost absent near the surface in the layer up to ~ 50 nm, which has the Si oxide, but the profile exhibits two peaks at 80 and 180 nm with the peak concentration $\sim 1.2 \cdot 10^{21}$ atoms/cm^3. Based on the given ratio of the dopant concentrations, it can be assumed that formation of the InAs phase is unlikely in this case.

Finally, we proceed to consideration of results of lamp annealing of second duration (the K5 sample, Fig. 6). It is clear in Fig. 6, *a* that the dopant peaks retain their initial shape as a whole, while demonstrating small tails of the distributions deep into Si. A slight level of channeling of the ions He^+ is present in both the peaks. The silicon range exhibits slight oxidation of the surface and a quite low degree of disordering, which are comparable to the characteristics of the K4a sample. As a result of such annealing in the solid-phase mode, the crystallinity degree of the Si layer gets the maximum value of 88.1 %, while the portion of the dopant atoms in the substitution position is 24.8 % (Table 2).

The experimental profiles of distribution of the concentration of In and As (Fig. 6, *b*) demonstrate peaks with the concentrations $\sim 3 \cdot 10^{21}$ atoms/cm^3 (As) and $\sim 5 \cdot 10^{21}$ atoms/cm^3 (In), which are mutually overlapped with a maximum of overlaps near 50 nm. At this depth, formation of the InAs phase is most likely. Besides, the profiles have tail portions that extend to 170 nm (In) and 210 nm (As). At this depth, formation of the solid solution Si:In (Si:As) is probable. In order to confirm the above-made assumptions in relation to formation of the nanoparticles of the InAs narrow-bandgap semiconductor in the Si matrix in a specific annealing method, further experiments are required, which shall involve methods that are sensitive to the phase composition, such as X-Ray Diffraction, Transmission Electron Microscope and Raman-Scattering Spectroscopy, which is a subject of further research.

Conclusion

The study has compared influence of the various types of thermal treatment of the Si single crystals (subsequently enriched with the ions In^+ and As^+ in order to synthesize the InAs narrow-bandgap semiconductor) on specific features of the structure and the dopant composition of the modified Si layer. Special attention is paid to the depth distribution of the concentration of the dopant atoms, their arrangement in the Si lattice and crystal perfection of the annealed Si layers. For analysis, Rutherford Backscattering of helium ions was applied. Based on the obtained data, we have found that the best restoration of the silicon crystal lattice disturbed by double ion implantation, without any signs of its oxidation is observed after pulsed ion annealing in the liquid-phase mode. But in this case, the concentration of the dopants In and As near the surface greatly differs. The best overlapping of the dopant profiles of In and As with the high concentration (above 10^{21} atoms/cm^3), which facilitates effective nucleation and growth of the InAs nanoparticles, is observed after pulsed laser annealing, furnace annealing at 800 °C and fast lamp annealing, when there is no great diffusion redistribution of the introduced dopants.

Acknowledgments

The authors would like to thank G.A. Novikova for pulsed ion annealing of the samples and B.F Farrakhova for lamp annealing of the samples.

Funding

The study was financially supported by the Russian Science Foundation (the project No. 24-29-00069, https://rscf.ru/project/24-29-00069/).

Conflict of interest

The authors declare that they have no conflict of interest.

References

[1] S. Zi. *Fizika poluprovodnikovykh priborov*: v 2-kh kn. (Mir, M., 1984), kn. 1.
[2] A. Luque, A. Martí, C. Stanley. Nat. Phot., **6**, 146 (2012). DOI: 10.1038/nphoton.2012.1
[3] Electronic source. *NSM Archive — Physical Properties of Semiconductors*. Available at: http://www.matprop.ru/
[4] Z. Mamiyev, N.O. Balayeva. Mater. Today Sustain., **21**, 100305 (2023). DOI: 10.1016/j.mtsust.2022.100305
[5] A. Rogalski. Rep. Progress Phys., **68**, 2267 (2005). DOI: 10.1088/0034-4885/68/10/R01
[6] F. Komarov, L. Vlasukova, W. Wesch, A. Kamarou, O. Milchanin, S. Grechnyi, A. Mudryi, A. Ivaniukovich. Nucl. Instrum. Meth. Phys. Res. B, **266**, 3557 (2008). DOI: 10.1016/j.nimb.2008.06.010
[7] L. Rebohle, R. Wutzler, S. Prucnal, R. Hubner, Y.M. Georgiev, A. Erbe, R. Bottger, M. Glaser, A. Lugstein, M. Helm, W. Skorupa. Phys. Stat. Sol. C, **14**, 1700188 (2017). DOI: 10.1002/pssc.201700188
[8] I.E. Tyschenko, V.A. Volodin, A.G. Cherkov, M. Stoffel, H. Rinnert, M. Vergnat, V.P. Popov. J. Luminescence, **204**, 656 (2018). DOI: 10.1016/j.jlumin.2018.08.057
[9] F. Komarov, L. Vlasukova, O. Milchanin, W. Wesch, E. Wendler, J. Zuk, I. Parkhomenko. Mater. Sci. Engin.: B, **178**, 1169 (2013). DOI: /10.1016/j.mseb.2013.07.011
[10] A.V. Dvurechenskii, G.A. Kachurin, E.V. Nidaev, L.S. Smirnov. *Impulsnyi otzhig poluprovodnikovykh materialov* (Nauka, M., 1982) (in Russian).
[11] F.F. Komarov, O.V. Mil'chanin, I.N. Parchomenko, P.V. Kuchinskii, A.E. Al'zhanova, M.A. Mokhovikov, E. Wendler. J. Engin. Phys. Thermophys., **97**, 745 (2024). DOI: 10.1007/s10891-024-02946-7
[12] R.I. Batalov, V.V. Bazarov, V.I. Nuzhdin, V.F. Valeev, H.A. Novikov, V.A. Shustov, K.N. Galkin, I.B. Chistokhin, F.F. Komarov, O.V. Milchanin, I.N. Parkhomenko. J. Appl. Spectr., **91**, 1225 (2025). DOI: 10.1007/s10812-025-01841-0
[13] M. Mayer. SIMNRA user's guide, Max-Planck-Institut für Plasmaphysik, 1997
[14] Electronic source. *The Stopping and Range of Ions in Matter*. Available at: http://www.srim.org/
[15] R.I. Batalov, E.A. Marfin, D.D. Zaitsev. Inzh. fiz. zhurn., **3** (v pechati) (2026) (in Russian).
[16] V.M. Glazov, V.S. Zemskov. *Fiziko-khimicheskie osnovy legirovaniya poluprovodnikov* (Nauka, M., 1967) (in Russian).

Translated by M.Shevelev